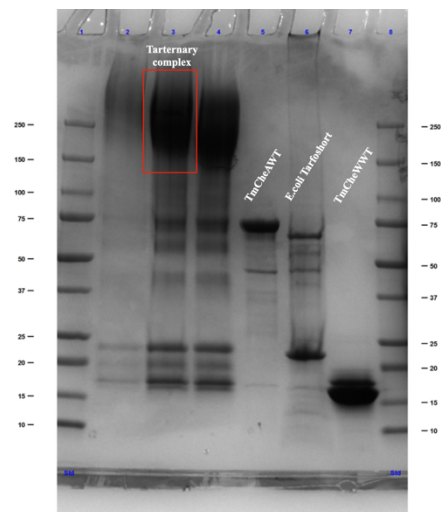
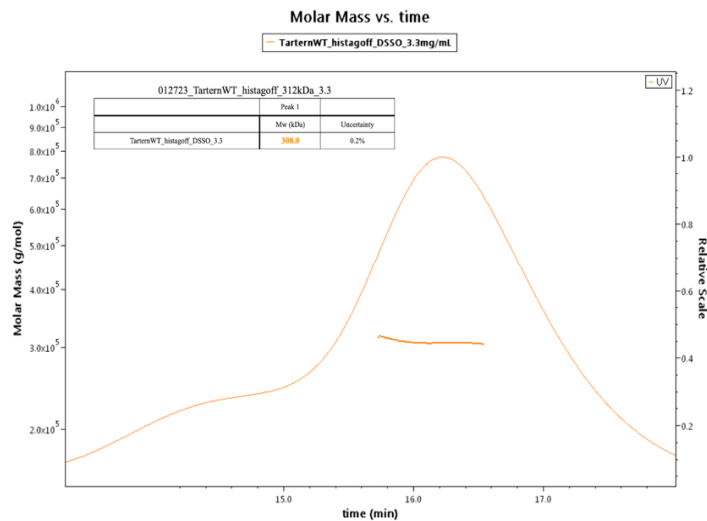


(A)



(B)



(C)

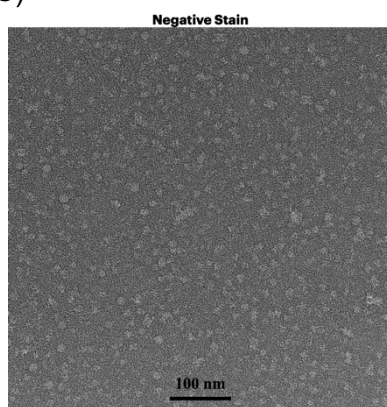
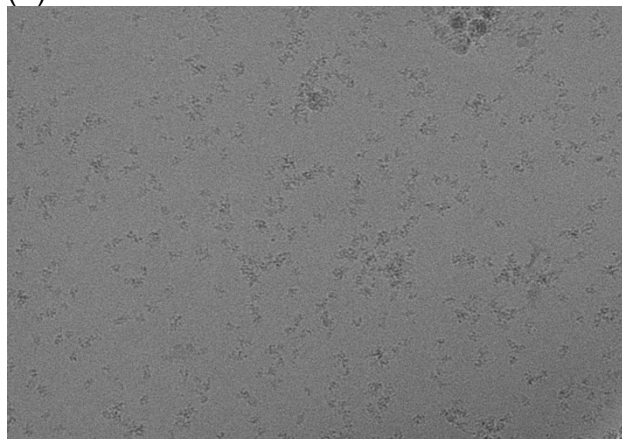
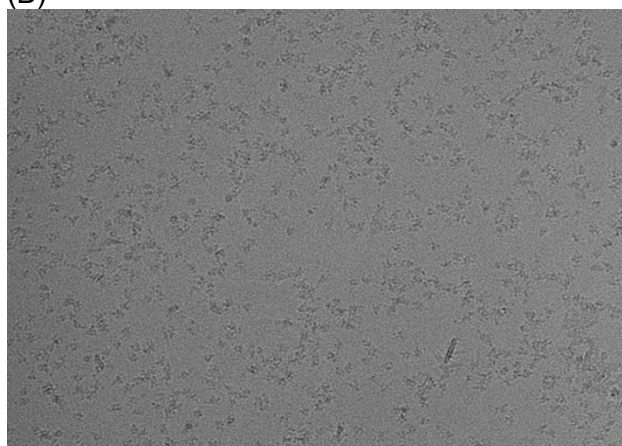


Figure 1: Negative Stain of the Tar ternary complex. (A) SDS page gel of purified TmCheAWT, TmCheWWT, and Tarfoldon_{short}, and the crosslinked Tar ternary complex. (B) SEC-MALS of DSSO crosslinked 3.3 mg/mL Tar ternary complex (C) Negative staining of 0.05 mg/mL Tar ternary complex using F200Ci.

(A)



(B)



(C)

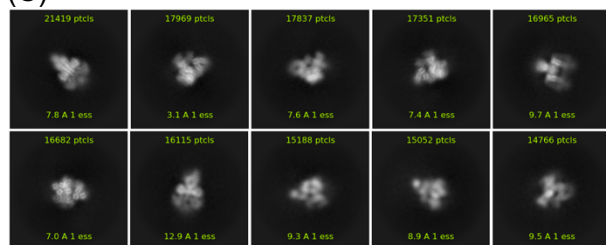
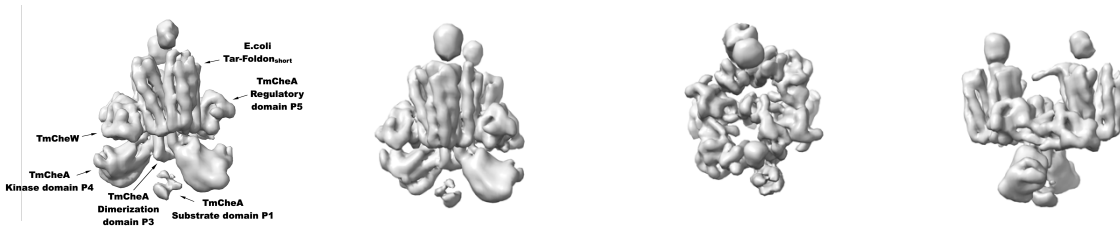
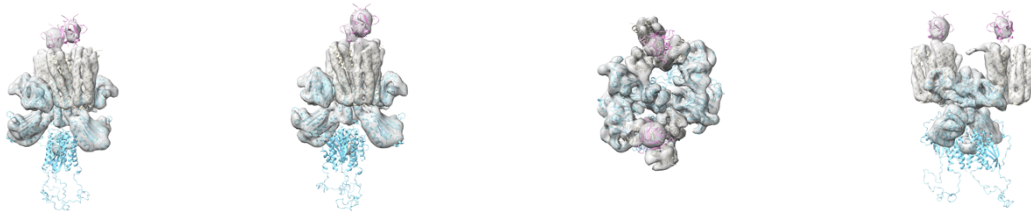


Figure 2: Cryo-EM of the DSSO-crosslinked Tar ternary complex (w/ TmCheAWT). (A) 3.5 mg/mL of Tar ternary complex with 2mM fos-choline-8 applied to Quantifoil Cu 1/2 grid. (B) 5.0 mg/mL of Tar ternary complex with 2mM fos-choline-8 applied to Quantifoil Au 1.2/1.3 grid. (C) Representative 2D classification of Tar ternary complex from ~900 micrographs and 476,981 particles that were collected on Auantifoil Cu 1/2 grid from (A). Topaz was applied for particle picking using CryoSPARC for the 2D classification of micrographs collected using 200 keV Arctica Talos with K3 detector (Gatan energy filter applied) from the Cornell Center for Materials Research (CCMR).

(A)



(B)



(C)



Figure 3: Preliminary 3D reconstruction of Tar ternary complex at 6.3 Å resolution from the CryoEM data set mentioned above. (A) Homogeneous refined 3D reconstruction at 6.3 Å resolution using cryoSPARC. (B) Map with superimposed model is based on (C) that determined by Muok et al. (Muok et al. *Science Signaling*, 2020).